Meteorological Aspects of the Sierra Wave

By Harold Klieforth

Meteorology Department, University of California at Los Angeles
(Present affiliation: Imperial College, London)

Presented at the 6th OSTIV Congress, St-Yan, France, July 1956

Introduction

The Sierra Wave is one of the more recently recognized, but by now one of the best known, examples of mountain lee waves. As it was with similar phenomena in Great Britain and Europe, sailplanes have played a leading role in both the discovery and exploration of the Sierra Nevada lee waves. An investigation of the air flow over the Sierra has been carried on since 1951 by the Meteorology Department of the University of California at Los Angeles under the sponsorship of the Geophysics Research Directorate. These studies included two field projects centered at Bishop in the Owens Valley of Eastern California. In the first of these, during the autumn and winter of 1951–2, a series of observations was made by instrumented sailplanes which were tracked from the ground, and in the second, in the spring of 1955, meteorological measurements were made also by powered aircraft flying at various altitudes across the Sierra. Kuettner (1955–6) has published some of the important results of the 1955 flights; in this paper are presented some results of the 1951–2 project.

Location and Plan of Observations

The topography. The Sierra Nevada is a single mountain range with a length of about 400 miles and a width varying from 50 to 80 miles (Fig. 1). Although the range extends roughly northwest-southeast between latitudes 35° and 40° North, the main crest of the High Sierra which borders on Owens Valley is only about 14° from a north-south orientation. In this southern portion of the range the crest is the highest, generally above 12,000 ft and with numerous peaks rising over 14,000 ft. There the eastern scarp is most abrupt, it is remarkably straight, and the Owens Valley, to the east at an average elevation of about 4,000 ft, is of nearly uniform width.

The east wall of Owens Valley is the large fault-block range known as the Inyo Mountains to the south of and the White Mountains to the north of 7,000 foot Westgard Pass. The Inyo Mountains have an average elevation of 9,000 to 11,000 ft, while the White Mountains, rivaling the Sierra in height, culminate in 14,254 foot White Mountain Peak just northeast

Fig. 1. Landforms of California. (Printed by courtesy of Ginn and Co.)

of Bishop. The western slope of these desert mountains is a fault scarp at the base of which the Valley reaches its lowest elevation. The floor of the eastern side of the Valley is fairly level but on the western side it rises in a broad alluvial apron to about 6,000 ft where it meets the steep flanks of the Sierra. In the central portion of the Valley near Independence—the region in which the aerial explorations of the Project were made—, the width of the Valley is about 10 miles and the distance from the crest of the Sierra to the crest of the Inyo Mountains is about 18 miles.

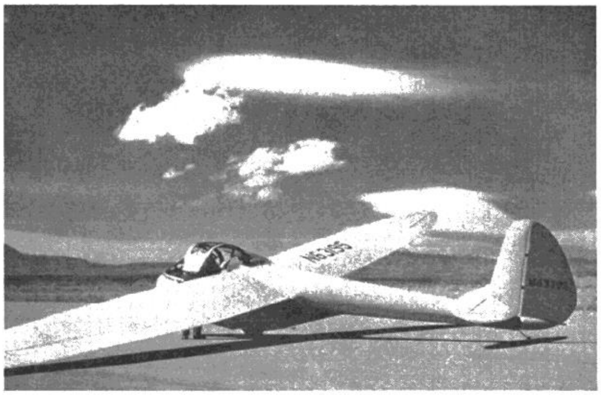

Fig. 2. A project sailplane at Bishop Airport

Sailplane tracking flights. In the fall and winter of 1951–2 sailplanes were tracked in flights in the lee flow of the Sierra by a network of 3 photo-theodolites, a radar set, and a Raydist system. Upwind, downwind, crosswind, and hovering runs and combinations of these were chosen to traverse the various parts of the lee wave flow according to their practicability under different wind and weather conditions. The Pratt-Read sailplanes used (Fig. 2) were two-place, had a wingspread of 50 ft, and a gross weight of about 1,400 pounds. The principal instruments borne by the sailplane were a clock, altimeter, rate of climb indicator, outside air thermometer, airspeed indicator, direction indicator, and accelerometer. The dials of these instruments in the panel of the sailplane were photographed at intervals of one or two seconds by 16 mm cameras mounted behind and to one side of the heads of the crew. Basic equipment of the sailplanes included a pressure oxygen breathing system, instrument-flight equipment, radio communication, barograph, and, for the crew, warm flying suits, parachutes, and oxygen masks. The ground tracking measurements of the 3 theodolites and the radar set were recorded as synchronous photographs at 5-second intervals of the corresponding time and instrument dial readings. The Raydist tracking data were recorded as brush recordings of the Raydist system's electronic signals.

Synthesis of Tracking and Airborne Data

Notation: In what follows these symbols and equations apply:

t	time
V_I	corrected indicated air speed
α	geographical heading in degrees (true north = 360°)
w_I	"indicated" sinking speed corresponding to V_I
T_I	indicated temperature + calibration correction
Z_I	indicated altitude
A	altimeter setting in inches of mercury
c_1	altimeter correction for instrument error and hysteresis
c_2	altimeter correction for static errors
Z_p	pressure altitude in the US Standard Atmosphere: $Z_p = Z_I + c_1 + c_2 + 925\ (29.92 - A)$
ϱ	density of air
ϱ_0	density at sea level corresponding to STP: 760 mm, 0° C
V_A	true speed of the sailplane with respect to the air: $V_A = V_I\ (\varrho_0/\varrho)^{1/2}$
w_A	sinking speed of the sailplane with respect to the air: $w_A = w_I\ (\varrho_0/\varrho)^{1/2}$
T	corrected free air temperature: $T = T_I + 0.85\ (V_A/100)^2$
$\underset{\sim}{V_A}$	horizontal velocity of the sailplane with respect to the air
Z	geometric altitude above mean sea level
$P\ (x, y, Z, t)$	position of sailplane determined by tracking system from origin O at Independence with x east and y north
$\underset{\sim}{V_G}$	velocity of sailplane with respect to the ground
$\underset{\sim}{V_H}$	horizontal component of the wind velocity: $\underset{\sim}{V_H} = \underset{\sim}{V_G} - \underset{\sim}{V_A}$
V_H	horizontal wind speed: $V_H = \lvert\underset{\sim}{V_H}\rvert$
x', y'	coordinates of reference system rotated and translated to origin O' on Sierra crest; x' along 70°, y' along 340°
β	angle between $\underset{\sim}{V_H}$ and the x' axis
U	horizontal wind speed component along x': $U = V_H \cos\beta$
w_G	vertical speed of the sailplane with respect to the ground: $w_G = (dZ/dt)_s \cong (dZ_p/dt)_s$
s	as a subscript it refers to quantities measured along the flight path
w	vertical wind speed: $w = w_G - w_A$
ε'	slope of streamline in exaggerated cross section: $\varepsilon' = \arctan 3wU^{-1}$
Δz	spacing of streamlines in the vertical: $\Delta z = C\ (\varrho U)^{-1}$
C	constant
p	pressure
R_d	gas constant for dry air: $R_d = 287$ kj per ton per °K
Θ	potential temperature in °K: $\Theta = T\ (100/p)^{2/7}$
D	"altimeter correction": $D = Z - Z_p$

The biggest task of the project was the reduction of the tracking data. The procedures for both the theodolite and Raydist records proved to be surprisingly complex and the computations were performed on an electronic computer. However, the details of this work do not concern us here and it suffices to state that the results in terms of the space positions $P\ (x, y, Z, t)$ were combined with the corrected sailplane measurements t, Z_p, α, V_A, w_A and T in the manner outlined briefly below to form the basic meteorological fields for analysis.

For comparison with theory, hydrodynamical models, and other lee wave observations it was important to obtain a synoptic picture of the air flow in the vertical plane perpendicular to the mountain range. The field of motion was thus analyzed in the form of streamlines in the plane perpendicular to the Sierra crest in the Independence tracking area. In order that these results can be considered as representing "synoptic" conditions, two assumptions are implied: 1) There was a steady state or $\partial/\partial t = 0$; and 2) the flow was two-dimen-

4098

sional, i. e., $\partial/\partial y' = 0$ where y' is the coordinate parallel to the Sierra crest.

The horizontal wind. On the horizontal chart of the flight path $\widehat{V_G}$ was measured graphically for overlapping 50 second intervals. On the sailplane computation sheets $\widehat{V_A}$ was determined for the same intervals as $\widehat{V_G}$, then subtracted graphically from $\widehat{V_G}$ to obtain $\widehat{V_H} = \widehat{V_G} - \widehat{V_A}$. The horizontal wind component perpendicular to the Sierra crest in the tracking area was obtained from $\widehat{V_H}$ by the formula $U = V_H \cos \beta$.

Vertical motion. On a time section $(dZ/dt)_s = w_G$ was computed graphically from the slope of the Z, t curve. From the sailplane computation sheets the values of w_A were plotted on the time section and added graphically to (subtracted algebraically from) w_G to obtain $w = w_G - w_A$ and thus a curve of w, t.

Streamlines. A continuous record of w, t then was had for all periods of continuous airborne measurements, and computations of U, t for periods of essentially straight flight for which both airborne and tracking data existed. In the cross section to be analyzed the vertical scale was exaggerated over the horizontal by 3 : 1 so that the exaggerated slope of the streamlines was plotted as the angle $\varepsilon' = \arctan 3w/U$. In order that the streamlines should represent the speed as well as the direction of the wind component in the (x', Z)-plane, the vertical spacing of the streamlines was made to vary inversely as the speed according to the formula $\Delta z = C\ (\varrho U)^{-1}$. The constant C chosen depended on the average speed of the wind for each lee wave but, of course, was kept constant for each flight. From the values of ε' and Δz the streamline analysis was then performed as an objective attempt to best satisfy the requirements of the data.

Other variables. From Z_p, p was obtained directly from Bellamy's (1945) tables, and from p and the corresponding T were computed density ϱ and potential temperature Θ by the formulas $\varrho = p\ (R_d T)^{-1}$ and $\Theta = T\ (100/p)^{2/7}$ where p is in cb and T and Θ are in °K. On the time section the values of $D = Z - Z_p$ were obtained graphically from the smoothed curves of Z and Z_p.

Vertical Cross Sections

Lee wave types. From all of the project observations one can classify the various types of lee waves observed over Owens Valley into three groups with the following characteristics:

Wave type	L (miles)	ζ (ft)	w (ft s^{-1})
Weak	2.5— 5	300—1,000	4—15
Moderate	5— 8	1,000—2,000	15—30
Strong	8—20	2,000—4,000	30–60
	(km)	(m)	(m s^{-1})
Weak	4— 8	100— 300	1— 5
Moderate	8—13	300— 600	5—10
Strong	13—32	600—1,200	10—20

L = the wavelength, ζ = the maximum displacement of a streamline from its undisturbed level or the wave amplitude, and w = the maximum vertical wind speeds.

In the above list the lower limit of wave length has been placed at 2.5 miles (4 km) since shorter waves than these are associated with individual ridges and peaks rather than with the main crest of the Sierra. At the other extreme, the longest wave observed was of the order of 20 miles (32 km) in wavelength so that the first wave crest lay over the Inyo Mountains—but this was a rare case. In some strong lee waves vertical speeds as high as 100 ft s^{-1} (30 m s^{-1}) have been encountered but the values given above are considered to be representative of the near-steady state flow. Three examples, one of a moderate wave and two of strong waves, from the 1951–2 season are presented below.

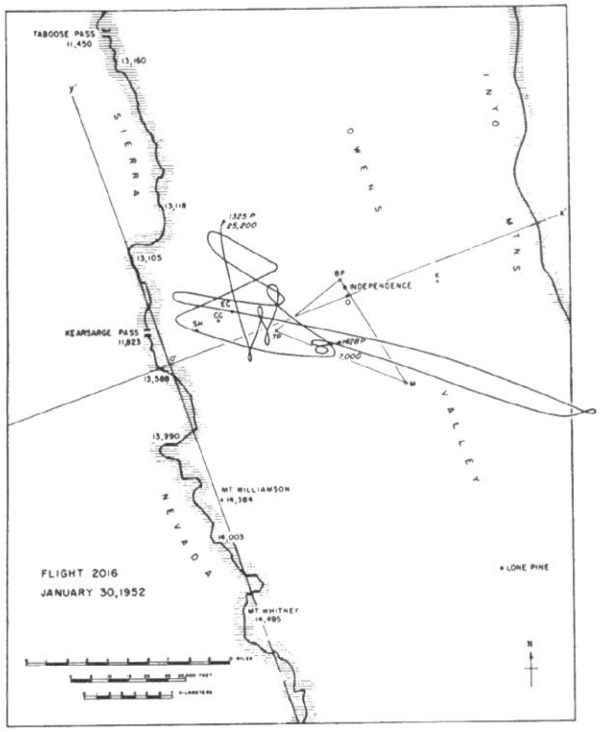

Fig. 3. Horizontal path of Flight 2016

Case 1. Flight 2016, 30th January 1952: a moderate lee wave

The wave was marked in the clouds by lenticular-form altocumulus arches with clear-cut leading edges over the Owens Valley. The sailplane was released from tow at 17,000 ft and reached a maximum altitude of 26,000 ft at which point tracking was begun. The flight path (Fig. 3) performed in the west-northwest flow included a criss cross run, a long downwind run through three complete wave lengths, and an upwind run prior to descent.

The flow pattern shown in Fig. 4 is that of a moderate wave in which three waves formed over the Owens Valley with an average wave length of 25,000 ft (8 km). The maximum displacement ζ was of the order of 1,200 ft. The constant used

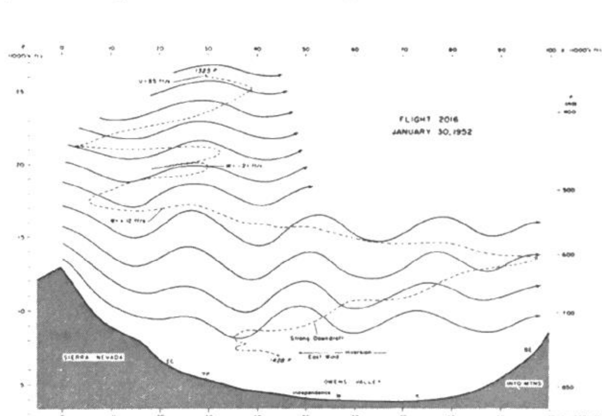

Fig. 4. Vertical cross section of Flight 2016 showing flight path and streamlines

in measuring streamline spacing was 5. The maximum U measured was 85 ft s^{-1} (50 knots). Maximum vertical velocities were +12 and —21 ft s^{-1} at the locations indicated on the cross section. In the lowest extent of the flight path, near 7,000 ft, a light easterly flow was measured. This suggested that below the wave crests between 7,000 and 9,000 ft were light rotor-like circulations which, however, are not to be confused with the so-called rotors of stronger waves that form at higher altitudes and are usually marked by roll (rotor) clouds. In this case there was neither enough moisture nor sufficient amplitude of the flow to induce the formation of clouds at the crests of the waves. Only at a higher level, perhaps 30,000 ft, was there a cloud which formed in the principal wave crest.

Fig. 5. Wave clouds in view south from Bishop on 16[th] February 1952. On the right is the Sierra partly hidden by the cloudfall. Above the large roll cloud is a deck of lenticular cloud

Case 2. Flight 2018, 16[th] February 1952: a strong lee wave

A photograph of the cloud phenomena of this day is shown in Fig. 5. The data from this flight are the most complete of all the flights and are of especial interest for the study of a strong lee wave with roll clouds. The tracking began at 1217 PST (Fig. 6) with an upwind run on tow and release was made in the strong updraft at 14,200 ft above 7P station. About that time the sailplane was lost to view by the theodolites because of the intervening roll cloud but its 45-minute ascent to a maximum altitude of 33,000 ft was followed by the Raydist system. A downwind and an upwind run were performed between 1344 and 1400 PST after the sailplane hand again been

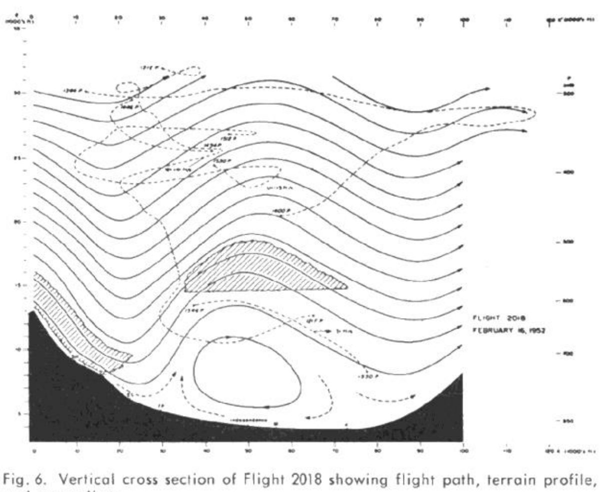

Fig. 6. Vertical cross section of Flight 2018 showing flight path, terrain profile, and streamlines

sighted by the theodolites. Later a criss cross run was tracked except for a gap during which the sailplane was above the roll cloud. The final run was made downwind under the roll cloud. The flight time from beginning to end of tracking data was $3^1/_2$ hours.

The air flow pattern of the lee wave is shown in Fig. 6 where $C = 7.5$. The wave length of the flow measured from trough to trough is 67,000 ft (20 km) at $Z = 15,000$ ft. The maximum amplitude ζ is 3,500 ft (1,100 m). Maximum vertical velocities measured along the flight path were +41 and —31 ft s^{-1} at the locations shown on the cross section. The maximum U measured on the flight was 115 ft s^{-1} (68 knots) near 24,000 ft at the point indicated. Measuring ε' and Δz along a vertical at $x' = 32,500$ ft through the inflection point of the flow upwind of the wave crest, and computing U and w from the formulas $U = C\ (\varrho \Delta z)^{-1}$ and $w = U/3 \tan \varepsilon'$, maxima of U are found to occur at $Z = 15,750$ ft where $U = 100$ ft s^{-1} (59 knots) and at $Z = 27,550$ ft where $U = 96$ ft s^{-1} (57 knots). Along the same vertical a single maximum of $w = 28$ ft s^{-1} is found at $Z = 15,250$ ft near the leading edge of the roll cloud.

The streamline of maximum amplitude passes through the center of the roll cloud but its mean altitude, that at the inflection points of the flow, is 13,500 ft. That the streamline of maximum amplitude should occur at a lower mean altitude than the altitude of the maximum vertical speed is a result of the dependence of the former on the maximum slope of the streamlines $\varepsilon = wU^{-1}$ rather than on w alone. A large positive vertical shear in the U profile through the roll cloud gives a rotor-like character to the *relative* circulation in and about the stationary roll cloud. Negative values of U are found under the roll cloud between the ground and about 8,000 ft—well below the base of the cloud.

Of interest are the synoptic variations of wind speeds between troughs and crests at different levels as measured along the path of the flight in Fig. 6. In the levels above the roll cloud zone the wind speed is least in the trough and greatest in the crest of the flow. Near 300 mb the speed varied from 21 m s^{-1} at the first lee trough to 31 m s^{-1} at the crest to 21 m s^{-1} at the second trough. Near 400 mb a similar difference is found; the speed varies from 24 m s^{-1} at the trough to 34 m s^{-1} at the crest. In the levels below the roll cloud the wind speed is greater in the troughs than in the crests as can be seen by comparing the streamline spacing at the troughs and the crests in those levels. The horizontal wind speeds and values of the other synoptic fields measured at critical points in the vertical plane are listed in Table 1 and discussed further below.

With reference to the values of T and Θ listed in Table 1, it is found tha the lowest temperature occur in the crests at all levels and the isolines of potential temperature approximate the streamline pattern as should be expected if the temperature changes along a streamline are adiabatic and the lapse rate is less than the dry adiabatic lapse rate.

Significant values of D measured along the flight path are given in the table. In the higher levels near 300 mb, D values appear to be highest in the troughs and lowest in the crest although one should temper this conclusion with the observation that since the points are not quite at the same level, there is undoubtedly some influence by the vertical hydrostatic gradient of D. However, the differences, of the order of 100 ft and corresponding to about 1.2 mb, are in close agreement with the observed acceleration of the wind from trough to crest at that level. The D values measured directly below the roll cloud at the crest of the flow appear to be somewhat greater than those in either updraft or downdraft, but this result is somewhat inconclusive because of differences in elevation of the points and the consequent effect of the vertical gradient of D.

 4100

Table 1. Flight 2018, 16th February 1952

Time PST	Position	Z ft	x' ft	p mb	T °C	Θ °K	w m s^{-1}	U m s^{-1}	D^* ft
1345	1st trough	29,790	20,200	304	—46.5	319	0	21	0
1348	wave crest	30,400	54,500	294	—51.0	316	0	31	—120
1350	2nd trough	28,800	86,800	319	—44.5	317.5	0	21	+ 80
1521	1st trough	(23,450)	18,000	402	—32.0	313.5	0	24	—
1525	wave crest	(23,400)	56,000	403	—33.0	312	0	34	—
1217	downdraft	12,420	62,200	632	— 7.0	304	— 5	9	—55
1220	wave crest	10,830	47,100	674	— 4.5	301	0	4	0
1223	updraft	11,070	32,600	665	— 5.0	302	+ 7	12	—110
1547	wave crest	14,170	45,500	589	—15.0	300.5	0	13	—100
1549	downdraft	11,000	65,400	669	— 5.5	300.5	—10	15	—40

* At some points D is indeterminate because no independent value of Z was computed, the position in those cases having been determined by Raydist or by one theodolite.

Upwind conditions at Merced, California, are shown in Fig. 7. The sounding shows rather moist air up to 400 mb and a stable lapse rate with one inversion near 650 mb (12,000 ft) and another near 480 mb (19,000 ft). The tropopause is at 218 mb (36,800 ft) with a temperature of —60° C. A stratospheric inversion has a maximum temperature of —49° C. The wind profile shows a rather strong shear to 25,000 ft above which the geostrophic speed appears to be nearly constant.

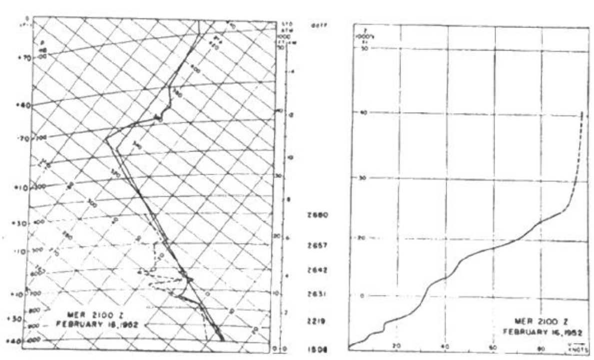

Fig. 7. Sounding and wind profile at Castle Air Force Base, Merced, California on 16th February 1952

Case 3. Flight 2006, 18th December 1951: a strong lee wave

As this flight was not tracked, a conventional streamline analysis was impossible. However, by invoking the assumption of adiabatic flow, it was possible to construct a potential temperature cross section which may be regarded as an approximate representation of the flow pattern in the (x', Z)-plane. Fig. 8 shows the cross section constructed from the 1000 PST radiosonde ascent from Lodgepole on the western slope of the Sierra and the "sounding" from Flight 2006; since the flight data used were measured in the period 0930 to 1045 PST, these were nearly synoptic. The Lodgepole sounding was plotted according to its calculated downwind drift with height and the sailplane measurements were plotted according to the path of the flight as reconstructed from the observer's notes. From photographs and observational notes the cap cloud (föhnwall), cloudfall, roll cloud, and lenticular cloud were sketched. It was assumed that the inversion of the föhnwall was the same as that of the roll cloud and that the air flow was isentropic except within the clouds. A rough calculation of the slope of the streamlines was made from the ration of the vertical wind speed $w = (dZ_p/dt - w_A)$ to the horizontal wind speed (equal to V_A in hovering flight). The wave length of the flow can be seen to vary from 46,000 to 59,000 ft (14 to 18 km or 9 to 11 miles). Note that the spacing of the isentropes indicates the stability rather than the wind speed.

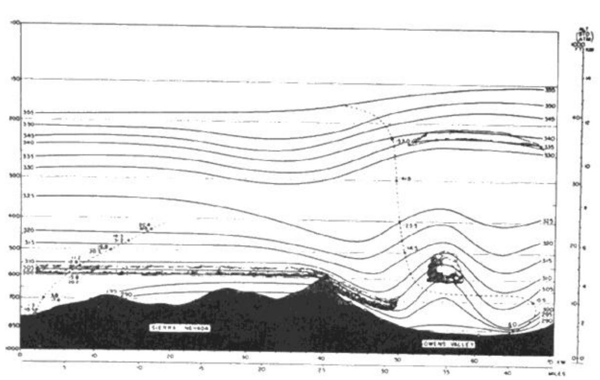

Fig. 8. Vertical cross section of potential temperature over the Sierra near 1000 PST on 18th December 1951

In the course of the ascent a maximum U of 85 knots was found at 24,000 ft. Maxima of w occurred in the roll cloud layer ($\pm$ 70 ft s^{-1}) and at about 32,000 ft ($\pm$ 40 ft s^{-1}). Severe turbulence was encountered near the roll cloud and again at about 31,000 and 39,000 ft. The maximum updraft area tilted upwind with height; drifting eastward at 38,000 ft the sailplane lost altitude above the region in which updrafts were encountered in lower levels and it was necessary to head westward with altitude in order to remain in the lift area. Of interest in the drawing is the suggestion of a much longer wave length in the stratosphere, a phenomenon that was nicely detected by the B-47 measurements over the Sierra in the strong lee wave of 1st April 1955 as reported by Dr. Kuettner (1955-6). On the return flight the wind speeds had increased by about 15 knots at 24,000 ft and reached an estimated maximum of 120 knots near 32,000 ft.

Summary of meteorological results. Besides the lee wave characteristics given at the beginning of this section, the following principal conclusions were drawn from all of the vertical cross sections and upwind soundings studied:

1) In strong lee waves without appreciable tilt the maximum wind speed in the horizontal occurs at the trough at levels below the roll cloud zone and at the crest at levels above the roll cloud zone. At a level in the roll cloud zone the vertical velocities appear to reach maximum values.

2) All of the cases of strong lee waves were associated with similar upwind temperature soundings with pronounced inversion layers whose tops lay between 12,000 and 19,000 ft altitude. The other lee wave cases of moderate and weak intensity were associated with varying degrees of stability in the

troposphere but generally without big inversion layers near mountain top level.

3) In the strong lee wave cases the wind profiles were similar with large vertical shear in the lower troposphere and with speeds increasing to maximum values of the order of 100 knots near 30,000 and 40,000 ft. Wind profiles for the moderate and weak lee wave examples showed lesser wind speeds at mountain crest level and lesser vertical shear in the troposphere.

4) The principal gradient of *D* value is that in the vertical due to the sounding being warmer or colder than that of the Standard Atmosphere. Significant horizontal differences in *D* are detectable only in strong waves. In none of the flights were large negative *D* values ("altimeter errors") measured.

5) The roll cloud which forms in the crests of the lee wave near or somewhat above the level of the mountain crest and often extends upward for several thousand feet, is turbulent in contrast to the laminar-like flow at higher levels. It is associated with the layer of strong stability and with a large positive vertical wind shear dU/dZ which gives a rotor-like appearance to the relative movements of the particles passing through the stationary cloud. Reverse flow frequently occurs in the lower layers near the ground and below the base of the roll cloud.

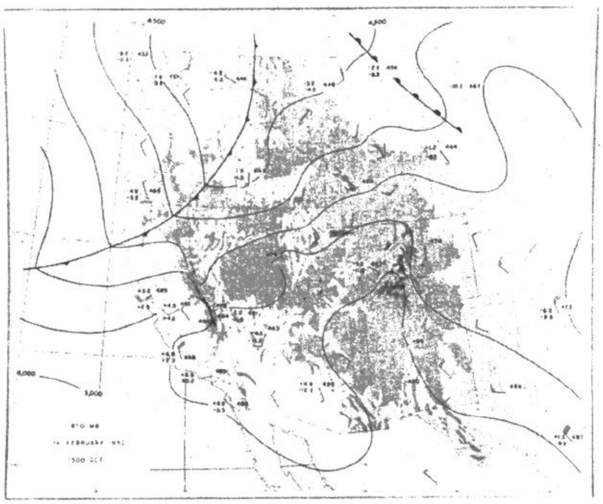

Fig. 9. 850 mb contour chart for 1500 GCT, 16[th] February 1952. Contour interval 100 ft., winds in knots, plotted figures are temperature and dew point in °C and contour heights

Synoptic Fields

One of the tasks of the Mountain Wave Project was to study the large-scale weather patterns in which lee waves were observed to occur. A set of upper air contour charts for 1500 GCT on 16[th] February 1952 (Case 2 above) are shown in Figs. 9, 10, 11, and 12. A cold front, the frontal trough, and the lee trough are pronounced features of the 850 and 700 mb contour patterns. Also of interest are the troughs in the lee of the Colorado Rockies and the Wind River Range in Wyoming. At 500 mb the flow over the Sierra was westerly with the frontal zone apparently over northern California and Idaho. The polar front jet stream at 300 mb was north of the Sierra at 1500 GCT but moved somewhat southward in the westerly current during the course of the day.

Considered as a whole, the principal results of the analyses of the large-scale synoptic fields associated with lee wave occurrences of the 1951-2 season were:

1) Strong lee waves are associated with: *a)* an upper trough along the Pacific Coast with strong westerly flow across the Sierra (large *T* and *D* gradients parallel to the coast); and

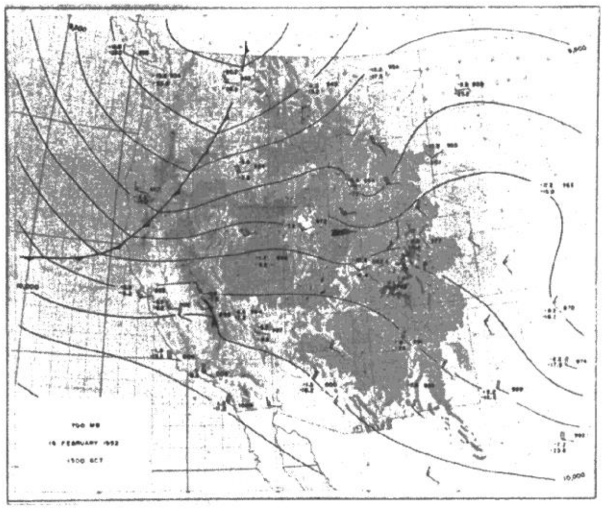

Fig. 10. 700 mb contour chart for 1500 GCT, 16[th] February 1952

b) a cold front or an occluded front approaching California from the northwest.

2) The soundings and wind profiles, which are the connecting links between the large-scale synoptic fields and the smallscale lee wave cross sections, are essentially pre-frontal in character. The high level inversion that forms the föhnwall and the roll clouds may be identified as a quasi-horizontal warm front.

3) The wave length of the large scale upper flow pattern affects the intensity of the lee wave and, in its effect upon the speed of the trough, it affects the duration of the lee wave phenomena. When the flow is strong and the wave length rather long, the strongest lee waves occur and persist for the longest period. When the wave length is comparatively short, the lee wave is of a more transitory nature.

Pressure Fields and Altimeter Errors

The pressure altimeter. The measurement of pressure in upper air soundings and the most generally used method for determination of the heights of aircraft both make use of the aneroid barometer. In the case of aircraft, the instrument is known as an altimeter and the readings are "indicated altitude" in accordance with the pressure-altitude relationship

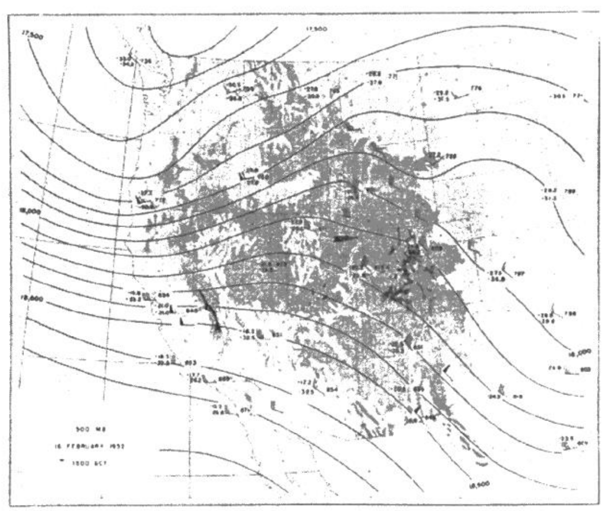

Fig. 11. 500 mb contour chart for 1500 GCT, 16[th] February 1952

defined by the US Standard Atmosphere. The most commonly used pressure altimeter is one in which one revolution of the principal pointer corresponds to 1,000 ft and in which a second pointer indicates thousands of feet, and a third the tens of thousands of feet. The instruments are calibrated for gross mechanical errors and usually there is some estimate of the corrections to be applied for dynamic pressure effects dependent on the speed and design of the various types of aircraft. An adjustable knob allows the pilot to change the "altimeter setting" and consequently the dial pointers in order that they may indicate the known geometric altitude of the airfield from which he is taking off. Similarly, before landing, the altimeter setting is radioed to the pilot in order that he will know the (nearly) exact indicated altitude at which the wheels of his aircraft will touch the ground. Most pilots have cognizance of the fact that the appropriate altimeter setting for indicating true altitude changes much more with altitude than from one altimeter setting station to the next, but, in general, this correction is not applied in routine flights; the problem of terrain clearance, to which this effect has particular relevance, is ostensibly solved by specifying a minimum flight altitude over mountains. In a rather definitive study of altimeters, the Operations and Engineering Group of the International Air Transport Association has issued a report (1953) on the various errors involved in pressure-altitude measurement. The magnitudes of the various known errors have been carefully estimated for different altitudes and for different specific uses of altimeters such as terrain clearance en route. The estimated maximum errors for the latter use are given in Table 2 below.

Table 2. Terrain clearance en route

Height (1,000's ft)	1,	3,	6,	10,	15,	22,	30,
Mechanical errors							
a) Diaphragm and							
b) Hysteresis	50	50	65	100	150	220	300 ft
c) Friction	20	25	30	30	45	55	75
d) Temperature	5	5	10	10	10	10	10
e) Backlash	10	10	10	10	10	10	10
f) Balance	20	20	20	20	20	20	20
g) Coordination	25	25	25	25	25	25	25
h) Instability	30	30	35	40	45	55	75
Operational errors							
a) Static system *	0	0	0	0	0	0	0
b) Zero setting	0	8	15	15	15	15	15
c) Readability							
i) Height scale	10	10	10	10	10	10	10
ii) Pressure scale	15	15	15	15	15	15	15
Principle errors							
a) Density (3 %)	30	90	180	300	450	660	900
b) Pressure datum	200	200	200	200	200	200	200
Maximum correction	±415	488	615	775	995	1295	1655 ft

Note: If the cruising level has been maintained for at least half an hour, the diaphragm and hysteresis correction could be reduced by 30 ft above 10,000 ft.

* Correction should be applied for this error.

From the above tables it is seen that the most serious errors are: the combined diaphragm and hysteresis errors, density errors (due to the atmosphere being warm or cold relative to the Standard Atmosphere), and pressure datum (altimeter setting) errors. At 15,000 ft, just above the peaks of the Sierra, the total error possible is of the order of 1,000 ft.

The lee wave pressure field. It has been recognized for many years that mountain waves, like thunderstorms, are among the phenomena excepted from the general assumption that pressures measured in the atmosphere reflect only hydrostatic conditions. In these exceptions to hydrostatic conditions the deviations of true pressures from pressures resulting solely from the "weight" of the air plane caused by vertical accelerations in the air flow. The principal difference between the non-hydrostatic pressures in lee waves and those in thunderstorms and related phenomena is that in the latter the vertical motion and its pattern of accelerations are rather unsystematic and non-steady whereas in the former they are systematic and approximate a steady state. Therefore, if the synoptic streamline pattern of a lee wave is known, it is possible to calculate the effect of the vertical velocity accelerations on the pressures measured by aircraft. In lee waves the maximum vertical accelerations occur at the trough and crest lines and are due to the curvature of the flow. The appropriate formula derived from the equation of motion for the pressure difference between two levels Z_0 and Z_1 on non-tilting trough or crest lines is:

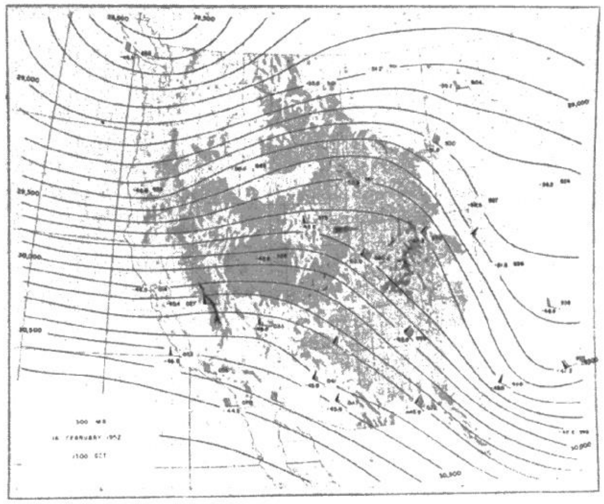

Fig 12. 300 mb contour chart for 1500 GCT, 16th February 1952

$$p_0 - p_1 = \int_{Z_0}^{Z_1} \varrho \, (g + U^2/R) \, dZ \qquad (1)$$

where g is the acceleration of gravity and R is the radius of curvature of the flow.

Now at trough and crest lines $U^2/R = U \, \partial w/\partial x$ and for periodic flow $\partial w/\partial x = \pm w_{max} 2\pi L^{-1}$ at trough and crest lines respectively where w_{max} is the vertical wind speed at the inflection point and L is the wavelength. Equation (1) can then be written in the practical form:

$$p_0 - p_1 = \int_{Z_0}^{Z_1} \varrho \, g \, dZ \pm \overline{\varrho \, U \, w_{max}} \, 2\pi \, L^{-1} \Delta Z \qquad (2)$$

where the bar denotes the average value and the plus sign applies at troughs and the minus sign at crests. This equation states that the difference in atmospheric pressure measured along a vertical between level Z_0 and a higher level Z_1 is equal to the hydrostatic pressure, i. e. the weight of air in the column of unit cross section, plus the integrated effect of the vertical centrifugal accelerations. It is apparent that the critical regions where both terms on the right side reach maximum values at any level are the troughs and crests of the vertical streamline pattern. Considering first the hydrostatic term, wherever the lapse rate is less than the adiabatic lapse rate, and assuming that the only temperature changes of air parcels in the wave flow are adiabatic, temperatures in the crest will be coldest and those in the troughs warmest at any level. This difference would lead to a horizontal pressure gradient from trough to crest which in a non-tilting wave would increase with height. Now the vertical acceleration term of (2) has the opposite effect in steady flow. The vertical centrifugal accelerations which are positive at the trough and negative at the crest, tend to make the air "heavier" at the trough and "lighter" at the crest and thus act to reduce the horizontal hydrostatic pressure gradients in lee waves. This result is not surprising since, from a physical point of view, it is the balance between hydrostatic and hydrodynamic forces which determines the flow characteristics.

If one considers the potential temperature cross section over the Sierra at 1000 PST on 18th December 1951 (Fig. 8) and computes hydrostatic pressure-height values along the verticals above barograph stations EC (through the trough) and M (through the crest), the 800—300 mb thickness of the trough is found to exceed that of the crest by 670 ft. (At 800 mb the hydrostatic D values of the two columns are equal.) To obtain a rough estimate of the total effect of the vertical accelerations of the streamline field in the layer from 800 to 300 mb, and recalling the large vertical speeds encountered by aircraft on that day, the following calculation is made in meter-ton-second units:

$$\begin{aligned} \Delta p &= \pm \overline{\varrho U w_{max}}\, 2\pi L^{-1} \Delta Z \\ &= \pm (0.75 \times 10^{-3})\,(30)\,(10)\,(2\pi)\,(^1/_{16} \times 10^{-3})\,(7{,}200) \\ &= \pm 0.64 \text{ cb} = \pm 6.4 \text{ mb} \end{aligned}$$

In applying this Δp to the entire layer one must use the average height difference this represents or that for about 500 mb which is 320 ft. Subtracting 320 ft from the hydrostatic height of the 300 mb surface over EC (trough) and adding 320 ft to the hydrostatic height of the 300 mb surface over M (crest), it can be seen that the total difference of 640 ft nearly equals the fictitious hydrostatic gradient of 670 ft from trough to crest at the 300 mb level.

Altimetry in flights over mountainous terrain. One of the most dramatic myths about the Sierra Wave is that concerning large altimeter errors of the order of 1,000 or even 2,000 ft associated with the disturbed air flow near the mountains. The alleged facts, widely circulated and widely believed, are based upon the stories of pilots who have flown in strong mountain waves and who have indeed noted significant differences between their altimeter reading and their apparent altitude. Project experience suggests that these «errors» are due to any of the three following causes listed in decreasing order of importance:

1. An upwind approach to the Sierra in which the pilot glances at his altimeter when near the trough of the wave just prior to encountering a 2,000 or 3,000 ft per minute downdraft and one minute later finds the aircraft approaching the mountain side at an altitude obviously 2,000 or 3,000 ft lower than intended. (If he were not so busy at the instant of comprehending this danger and had time to look at his altimeter, it would, in all probability, verify the unpleasant fact.)

2. A combination of large instrument errors—particularly diaphragm and hysteresis errors—in the altimeter used, operational errors (including static system), and large principle errors, particularly in air much colder than Standard Atmosphere and with an altimeter setting that is much too high for the region. The sum of all these at altitudes near the crest of the Sierra can be of the order of 1,000 ft (Table 2).

3. An optical illusion caused by either the lack of a horizon when flying under clouds in mountainous terrain or by a looming effect caused by refraction of light by a temperature inversion near the level of the mountain crest.

As for errors caused by the vertical accelerations in the lee wave, the computations and measurements indicate that these effects are smaller than the hysteresis errors and are therefore generally undetectable. It should be mentioned that in the non-steady flow in the roll cloud region of certain strong mountain waves, there are probably large vertical accelerations of short duration, but in such instances the associated turbulence is by far the greater hazard and concern over the slight effect on the altimeter is irrelevant.

The "one minute later effect" (1. above) is the real Lorelei of the mountain wave for pilots. Often the downdraft is so smooth as to be hardly perceptible if one were not watching either instruments or terrain; the aircraft is simply pushed rapidly and steadily toward the ground. The stronger the downdraft, the stronger are the horizontal winds and so an aircraft flying upwind requires more time to traverse the dangerous area. Also, the total loss of altitude will be even greater if the aircraft approaches the mountain range obliquely and will be at a maximum when flying parallel to the range along the downdraft area. The result of a minute's inattention and reliance on the automatic pilot in such conditions can be catastrophic.

Acknowledgements

It is not possible to name here all those who contributed so much to the Sierra Wave studies but great appreciation is felt for the endeavors of all those, particularly the members of the Southern California Soaring Association, who participated in the observational problem. Most of the analysis was carried out with Einar Hovind of the UCLA Meteorology Department. Grateful acknowledgement is given of the continued interest and many helpful suggestions afforded this work by Professors Jacob Bjerknes and Jörgen Holmboe of the UCLA Meteorology Department and by Dr. Joachim Kuettner of the Geophysics Research Directorate.

Note: The research reported on here was sponsored by the Geophysics Research Directorate, Air Force Cambridge Research Center under Contract AF 19 (122)—263.

References

John C. Bellamy, 1945: Journal of Meteorology, Vol. 2, No. 1.
Joachim P. Kuettner, 1955—56: Soaring, Vol. 19, Nos. 5, 6; Vol. 20, Nos. 1, 2. — Swiss Aero Revue, 1956, No. 6.
OPS-ENG Report, International Air Transport Association (1953).

4104